International Journal of GEOMATE, Aug., 2022, Vol.23, Issue 96, pp.1-10
ISSN: 2186-2982 (P), 2186-2990 (O), Japan, DOI: https://doi.org/10.21660/2022.96.3233
Geotechnique, Construction Materials and Environment

VERTICAL DYNAMIC RESPONSE OF A FRICTION PILE IN MULTILAYERED SOIL

Hiep Toan Luong[1] and *Hien Manh Nghiem[2]

[1]Department of Civil Engineering, HUTECH University, Vietnam; [2]Department of Civil Engineering, Hanoi Architectural University, Vietnam

*Corresponding Author, Received: 05 Jan. 2022, Revised: 21 Feb. 2022, Accepted: 12 June 2022

ABSTRACT: A semi-analytical-numerical method is developed to investigate the vertical dynamic response of a single pile embedded in multilayered soil. The governing differential equation for the pile and soil settlements is derived using the energy principles and variational approach that can consider both normal and shear strains in the vertical direction. The soil displacement in the vertical direction is expressed in terms of the pile displacement in the vertical direction and a decay function in the radial direction. The pile is modeled by a series of elements and the differential equation for each element is solved by applying the finite element method where exact shape functions are employed. The iterative algorithm is adopted to solve the pile settlement and the pile head impedance instead of solving simultaneously many equations and the proposed method is implemented in a computer code to obtain the solution. The validation of the proposed method is performed via a comparison of the pile head impedance and static stiffness with those from existing methods in the literature for both end-bearing and friction piles in homogeneous and multilayered soils. The pile head impedances calculated using the proposed method match well those obtained from approximate analytical solutions and are in good agreement with those from the three-dimensional finite element analyses at zero frequency.

Keywords: Friction Pile; Energy principle; Variational approach; Pile head impedance; dynamic axial load.

1. INTRODUCTION

Lateral dynamic loads such as earthquakes, and wind applied to high-rises transfer to pile foundation mostly in the vertical direction via overturning moment. The dynamic axial loads from machine vibrations and traffic are also applied vertically to the pile foundation. The pile head impedance represents the response of the pile foundation under harmonic load and is usually used in evaluating the dynamic behavior of soil-pile-structure interaction.

Several theoretical models were developed to investigate the dynamic interaction of the pile-soil system in the frequency domain in the literature. Novak [1] proposed a plane-strain model in which the soil is divided into a series of thin independent horizontal layers to analyze the dynamic response of an embedded cylindrical foundation. In the model, each thin soil layer is subjected to dynamic plane-strain deformation caused by vibration waves that s only propagate in the horizontal direction. The plane-strain model (a.k.a the Novak's method) was extensively used in pile dynamics [1-5] and modified to improve the dynamic response of the pile [4,5]. Lakshmanan and Minai [2] developed a solution for piles embedded in radially inhomogeneous soil under vertical, torsional, and lateral loads based on Novak's method. El Naggar [3] manipulated the k's method and obtained the same subgrade equation as Lakshmanan and Minai [2] for the pile under vertical load. Mylonakis [4] accounted for the horizontal shearing stress and vertical normal stress in the plane-strain model and solved for the end-bearing pile under vertical excitation. The solutions based on Novak's method [1-5] have the advantage that a dynamic subgrade reaction of the pile-soil system in viscoelastic layers with arbitrarily varying material properties can be obtained explicitly. Anoyatis and Mylonakis [5] derived an axisymmetric wave solution, based on linear elastodynamic theory, for the dynamic response of finite and infinitely long piles in a homogeneous viscoelastic soil with the former type of pile resting on rigid roa ck. The equilibrium of an arbitrary soil element in the vertical direction in these solutions [4,5] can yiyieldhethe conventional static plane-strain model of Randolph and Wroth [6] if the frequency of vibration is zero. The solutions [4,5] were only applied for end-bearing piles penetrated in homogeneous soil.

Rajapakse and Shah [7,8] and Rajapakse [9] developed a solution scheme based on Green's function representations for the surrounding half-space. Rajapakse [9] proposed the fictitious bar extended half-space to provide a consistent and accurate solution for axisymmetric elastodynamic load transfer problems over a wide range of frequencies of excitation. The solutions can be applied for friction piles, but only homogeneous

soil was considered, and the results were not verified for the static pile head stiffness as the pile head impedance at zero frequency without material damping.

Vallabhan and Mustafa [10] proposed the method based on the energy principles and variational approach (EPVA) for the pile embedded in homogeneous soils under vertical static load. The advantage of this continuum-based analysis is that it can capture the three-dimensional behavior of the pile-soil interaction and produce pile load-settlement responses in seconds. The method was adopted to solve for the pile in layered soils [11-13] under static vertical load. For example, Seo and Prezzi [11] proposed the explicit solution for a circular pile, Seo et al. [12] solved for circular and rectangular piles, and Salgado et al. [13] accounted for both vertical and radial soil displacements in the solution of the circular pile. Gupta and Basu [were applied this approach to solve for the end-bearing pile under vertical dynamic load. The solution algorithm did not provide more general problems such as a friction pile embedded in multi-layered soils.

2. RESEARCH SIGNIFICANCE

Presently, no solution is developed using the energy principles and variational approach for friction pile embedded in multi-layered soil under vertical dynamic load. This shortcoming is overcome in the proposed method in which the finite element method for bar element on elastic foundation using exact shape functions and the iterative solution is employed [15].

3. PILE-SOIL MODEL

A pile-soil system is subjected to vertically and laterally propagating waves during vertical excitations as shown in Fig. 1a. The pile with a circular cross-section is represented by geometrical and material properties such as radius r_p, length Young's modulus E_p, and density ρ_p. A dynamic load applies at the pile head and center of the cross-section in the vertical direction. The pile is embedded in a multilayered soil media with a total of n soil layers extending to infinite in the horizontal direction. The pile penetrates through m soil layers where the pile base is assumed to be located at the bottom of the m^{th} layer. The soil properties are denoted by subscript "s" for the general soil layer while the properties of the k^{th} soil layer are described by subscript "k" for the multi-layered soil. The pile and the soil column (below the pile tip) are modeled by a series of bar elements as shown in Fig. 1a. If soil properties vary with depth in each layer, the pile and soil columns are divided into several sub-elements and the properties are considered constants for each sub-element. The j^{th} element of length L_j (Fig. 1c) is surrounded by the k^{th} soil layer. A cylindrical coordinate is appropriate to use in the axisymmetric model as gloabal coordinate system, as shown in Fig. 1a where the origin is located at the center of the pile cross-section at the pile head. The coordinate system includes three axes: r-axis in the radial direction, Z-axis in the vertical direction, and θ-axis in the tangential direction, as shown in Figs. 1a and 1b. The Z-axis is positive in a downward direction coinciding with the pile axis. The coordinate z is considered athe s local coordinate of the jth element that varies from 0 to L_j.

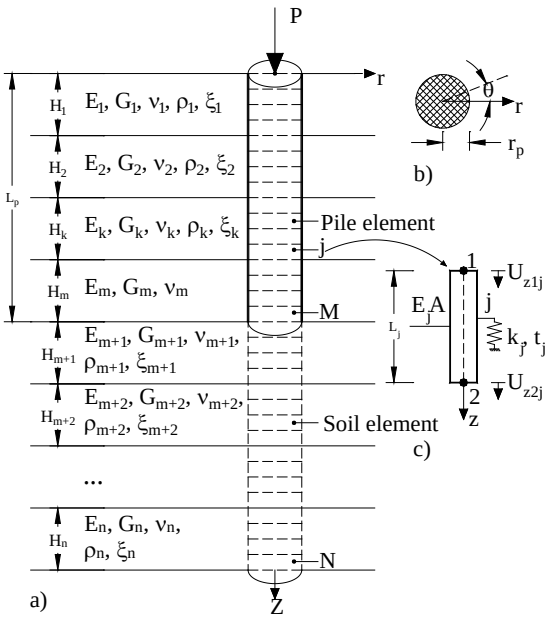

Fig. 1. Pile-soil system

The following assumptions are applied to the pile-soil system:

1) Tangential and radial displacements are very small compared to vertical displacement and hence can be assumed negligible.
2) The pile is single and vertical with a circular cross-section and isotropic linear elastic material. No slippage between soil and pile is allowed at the pile-soil interface then the displacements at the pile-soil interface meets compatibility requirement.
3) The soil is considered a viscoelastic and isotropic material.
4) No normal and/or shear tractions are applied at the surface of the soil media.

The kth soil layer with a thickness of H_k is represented by the complex-valued Lamé constants as follows [16]:

$$E_k^* = E_k\left(1+2i\xi_k\right)$$
$$G_k^* = G_k\left(1+2i\xi_k\right) \quad (1)$$
$$\lambda_k^* = \lambda_k\left(1+2i\xi_k\right)$$

where:

$i=\sqrt{-1}$; $\lambda_k = E_k \dfrac{\nu_k}{(1+\nu_k)(1-2\nu_k)}$; E_k is Young's modulus; G_k is shear modulus; ξ_k is damping ratio ; and ν_k is Poisson's ratio.

4. DISPLACEMENT-STRAIN-STRESS RELATIONSHIP

Since the vertical displacement in the radial direction decreases with the increase of radial distance from the pile, the vertical displacement field in the soil can be approximated by a product of separable functions as follows [10-13]:

$$u_z = U_z\phi \quad (2)$$

where U_z is the vertical displacement of the pile at a depth of z; ϕ is the dimensionless function of r describing the reduction of the displacement in the radial direction from the pile center. It is assumed that $\phi = 1$ at $r = r_p$, and $\phi = 0$ at $r = \infty$.

The vertical dynamic displacement is expressed in a form of harmonic excitation as:

$$U_z = \bar{U}_z e^{i\omega t} \quad (3)$$

where $\bar{U}_z$ is the amplitude of the vertical displacement; and ω circular frequency of vibration.

Velocity is the derivative of displacement versus time that can be obtained as:

$$v = \frac{du_z}{dt} = i\omega\bar{U}_z e^{i\omega t}\phi = i\omega U_z\phi \quad (4)$$

Inertial energy in the soil can be written in terms of velocity and soil density as the following equation:

$$\frac{1}{2}\rho_s v^2 = \frac{1}{2}\rho_s\left(\frac{du_z}{dt}\right)^2 = -\frac{1}{2}\rho\omega^2 U_z^2\phi^2 \quad (5)$$

With the above assumptions, the strain-displacement relationship can be expressed in terms of the displacement field as:

$$\begin{Bmatrix}\varepsilon_r\\ \varepsilon_\theta\\ \varepsilon_z\\ \gamma_{r\theta}\\ \gamma_{rz}\\ \gamma_{z\theta}\end{Bmatrix} = \begin{Bmatrix} -\dfrac{\partial u_r}{\partial r}\\ -\dfrac{u_r}{r}-\dfrac{1}{r}\dfrac{\partial u_\theta}{\partial\theta}\\ -\dfrac{\partial u_z}{\partial z}\\ -\dfrac{1}{r}\dfrac{\partial u_r}{\partial\theta}-\dfrac{\partial u_\theta}{\partial r}+\dfrac{u_\theta}{r}\\ -\dfrac{\partial u_z}{\partial r}-\dfrac{\partial u_r}{\partial z}\\ -\dfrac{1}{r}\dfrac{\partial u_z}{\partial\theta}-\dfrac{\partial u_\theta}{\partial z}\end{Bmatrix} = \begin{Bmatrix}0\\0\\-\phi\dfrac{dU_z}{dz}\\0\\-U_z\dfrac{d\phi}{dr}\\0\end{Bmatrix} \quad (6)$$

The following equation presents the relationships between stress and strain in the soil based on Hooke's law for isotropic linear viscoelastic material:

$$\begin{Bmatrix}\sigma_r\\ \sigma_\theta\\ \sigma_z\\ \tau_{r\theta}\\ \tau_{rz}\\ \tau_{z\theta}\end{Bmatrix} = \begin{bmatrix}\lambda_s^*+2G_s^* & \lambda_s^* & \lambda_s^* & 0 & 0 & 0\\ \lambda_s^* & \lambda_s^*+2G_s^* & \lambda_s^* & 0 & 0 & 0\\ \lambda_s^* & \lambda_s^* & \lambda_s^*+2G_s^* & 0 & 0 & 0\\ 0 & 0 & 0 & G_s^* & 0 & 0\\ 0 & 0 & 0 & 0 & G_s^* & 0\\ 0 & 0 & 0 & 0 & 0 & G_s^*\end{bmatrix}\begin{Bmatrix}\varepsilon_r\\ \varepsilon_\theta\\ \varepsilon_z\\ \gamma_{r\theta}\\ \gamma_{rz}\\ \gamma_{z\theta}\end{Bmatrix} \quad (7)$$

where σ is normal stress; and τ is shear stress.

5. GOVERNING EQUILIBRIUM EQUATIONS

The potential energy Π of the soil-pile system defined as the sum of internal energy and external energy can be expressed by following equation:

$$\begin{aligned}\Pi = &\sum_{j=1}^{N}\frac{1}{2}\int_0^{L_j} E_j^* A\left(\frac{dU_{zj}}{dz}\right)^2 dz\\ &+\sum_{j=1}^{N}\frac{1}{2}\int_0^{L_j}\int_0^{2\pi}\int_{r_p}^{\infty}\{\sigma\}^T\{\varepsilon\}\,r dr d\theta dz\\ &-\sum_{j=1}^{N}\int_0^{L_j}\int_0^{2\pi}\int_0^{r_p}\frac{1}{2}\rho_j\omega^2 U_{zj}^2 r dr d\theta dz\\ &-\sum_{j=1}^{N}\int_0^{L_j}\int_0^{2\pi}\int_{r_p}^{\infty}\frac{1}{2}\rho_k\omega^2 U_{zj}^2\phi^2 r dr d\theta dz\\ &-PU_{z_0}\end{aligned} \quad (8)$$

where E_j^* is Young's modulus of the j^{th} element, if $j \le M$ then $E_j^* = E_p^*$, if $j > M$ then $E_j^* = E_k^*$; ρ_j is mass density of the jth element; ρ_k is mass density of the kth soil layer; A is the area of the pile cross-section; U_{zj} is displacement of the j^{th} element; P and U_{z_0} are vertical dynamic load and

displacement at the depth $z = z_0$, respectively; $\{\sigma\}$ and $\{\varepsilon\}$ are the stress and the strain tensors.

Strain energy for the k[th] soil layer is obtained as:

$$\frac{1}{2}\{\sigma\}^T\{\varepsilon\} = \frac{1}{2}\left(\lambda_k^* + 2G_k^*\right)\left(\phi\frac{dU_z}{dz}\right)^2 + \frac{1}{2}G_k^*\left(U_z\frac{d\phi}{dr}\right)^2 \quad (9)$$

Equation (9) is derived from Eq. (6) and Eq. (7) with soil displacement in the radial direction is assumed to be zero. This assumption completely introduces artificial restraint in the radial direction in the pile-soil system that may produce significant effect on the response of the vertically loaded pile. The effect of restraint was reduced by Seo et al. [12] for pile under static load and Mylonakis [5] for pile under dynamic load by modifying the term of $\left(\lambda_k^* + 2G_k^*\right)$ in Eq. (9).

The potential energy can be obtained in the following equation by substituting Eq. (9) with Eq. (8), and integrating concerning θ:

$$\begin{aligned}\Pi = {} & \frac{1}{2}\sum_{j=1}^{N}\int_0^{L_j} E_j^* A\left(\frac{dU_{zj}}{dz}\right)^2 dz \\ & + \pi\sum_{j=1}^{N}\int_0^{L_j}\int_{r_p}^{\infty}\bar{E}_k^*\left(\phi\frac{dU_{zj}}{dz}\right)^2 r dr dz \\ & + \pi\sum_{j=1}^{N}\int_0^{L_j}\int_{r_p}^{\infty}G_k^*\left(U_{zj}\frac{d\phi}{dr}\right)^2 r dr dz \\ & - \frac{1}{2}\omega^2\pi r_p^2\sum_{j=1}^{N}\rho_j\int_0^{L_j}U_{zj}^2 dz \\ & - \omega^2\pi\sum_{j=1}^{N}\int_0^{L_j}\rho_k\int_{r_p}^{\infty}U_{zj}^2\phi^2 r dr dz \\ & - PU_{z_0}\end{aligned} \quad (10)$$

where $\bar{E}_k^* = \lambda_k^* + 2G_k^*$ is constraint modulus.

By minimizing the potential energy, or the first variation of the potential energy must be zero [10-13], the equilibrium equations of the soil and pile elements can be made as follows:

$$\begin{aligned}\delta\Pi = {} & \sum_{j=1}^{N}\left(\frac{\partial\Pi}{\partial U_{zj}} - \frac{d}{dz}\frac{\partial\Pi}{\partial U'_{zj}}\right)\delta U_{zj} \\ & + \left(\frac{\partial\Pi}{\partial\phi} - \frac{d}{dr}\frac{\partial\Pi}{\partial\phi'}\right)\delta\phi \\ & = 0\end{aligned} \quad (11a)$$

where $U'_{zj} = \frac{dU_{zj}}{dz}$ and $\phi' = \frac{d\phi}{dr}$

$$\begin{aligned}\delta\Pi = {} & \sum_{j=1}^{N}\left\{\int_0^{L_j}\left[\left(-E_j^* A - 2\pi\bar{E}_k^*\int_{r_p}^{\infty}\phi^2 r dr\right)\frac{d^2U_{zj}}{dz^2}\right.\right. \\ & + 2\pi G_k^*\int_{r_p}^{\infty}\left(\frac{d\phi}{dr}\right)^2 r dr U_{zj} - \pi r_p^2\rho_j\omega^2 U_{zj} \\ & \left.\left. - 2\pi\rho_k\omega^2\int_{r_p}^{\infty}\phi^2 r dr U_{zj}\right]dz\right\}\delta U_{zj} \\ & \left\{\int_{r_p}^{\infty}\left[-2\pi\sum_{j=1}^{N}G_k^*\int_0^{L_j}U_{zj}^2 dz\frac{d^2\phi}{dr^2}r\right.\right. \\ & - 2\pi\sum_{j=1}^{N}G_k^*\int_0^{L_j}U_{zj}^2 dz\frac{d\phi}{dr} \\ & + 2\pi\sum_{j=1}^{N}\bar{E}_k^*\int_0^{L_j}\left(\frac{dU_{zj}}{dz}\right)^2 dz\phi r \\ & \left.\left. - 2\pi\omega^2\sum_{j=1}^{N}\rho_k\int_0^{L_j}U_{zj}^2 dz\phi r\right]dr\right\}\delta\phi \\ & = 0\end{aligned} \quad (11b)$$

Equation (11) can be written in the form of:

$$\sum_{j=1}^{N}A\left(U_{zj}\right)\delta U_{zj} + B(\phi)\delta\phi = 0 \quad (12)$$

U_{zj} and ϕ satisfy equilibrium within each of the sub-domains ($0 \le z \le L_j$ or within the j[th] element for U_{zj}, and $r_p \le r \le \infty$ for ϕ) and hence, over the entire domain. The functions $A\left(U_{zj}\right)$ and $B(\phi)$ are unknown, δU_{zj} and $\delta\phi$ are not zero, one of the solutions for Eq. (12) can be obtained by assigning $A\left(U_{zj}\right)$ and $B(\phi)$ all equal to zero. The differential equation for the j[th] element can be obtained from $A\left(U_{zj}\right) = 0$ as follows:

$$\begin{aligned}& \left(E_j^* A + 2\pi\bar{E}_k^*\int_{r_p}^{\infty}\phi^2 r dr\right)\frac{d^2U_{zj}}{dz^2} \\ & - \left[2\pi G_k^*\int_{r_p}^{\infty}\left(\frac{d\phi}{dr}\right)^2 r dr\right]U_{zj} \\ & + \left[\pi r_p^2\rho_j\omega^2 + 2\pi\rho_k\omega^2\int_{r_p}^{\infty}\phi^2 r dr\right]U_{zj} = 0\end{aligned} \quad (13)$$

Equation (13) can be written in the short form as:

$$\left(E_j^* A + t_j\right)\frac{d^2 U_{zj}}{dz^2} - k_j U_{zj} = 0 \tag{14}$$

where k_j and t_j are subgrade reactions for shearing and axial resistances, respectively, and determined as:

$$k_j = 2\pi G_k^* \int_{r_p}^{\infty}\left(\frac{d\phi}{dr}\right)^2 r dr - \rho_j \omega^2 \pi r_p^2 - 2\pi\rho_k \omega^2 \int_{r_p}^{\infty}\phi^2 r dr \tag{15}$$

$$t_j = 2\pi \bar{E}_k^* \int_{r_p}^{\infty}\phi^2 r dr \tag{16}$$

Applying the principle of minimum potential energy and taking a variation of ϕ, the governing differential equation for the soil is given by:

$$\frac{d^2\phi}{dr^2} + \frac{1}{r}\frac{d\phi}{dr} - \frac{b}{a}\phi = 0 \tag{17}$$

where:

$$a = \sum_{j=1}^{N} G_k^* \int_0^{L_j} U_{zj}^2 dz \tag{18}$$

$$b = \sum_{j=1}^{N} \bar{E}_k^* \int_0^{L_j}\left(\frac{dU_{zj}}{dz}\right)^2 dz - \omega^2 \sum_{j=1}^{N}\rho_k \int_0^{L_j} U_{zj}^2 dz \tag{19}$$

Equation (17) can be rewritten as:

$$\frac{d^2\phi}{dr^2} + \frac{1}{r}\frac{d\phi}{dr} - \beta^2\phi = 0 \tag{20}$$

where:

If $b > 0$ then

$$\beta = \sqrt{\frac{b}{a}} \tag{21a}$$

If $b < 0$ then

$$\beta = i\sqrt{-\frac{b}{a}} \tag{21b}$$

The differential equation (20) is a form of the modified Bessel differential equation, and its solution is given by:

$$\phi = c_1 I_0\left(\beta r\right) + c_2 K_0\left(\beta r\right) \tag{22}$$

where I_0 is a modified Bessel function of the first kind of zero-order; K_0 is a modified Bessel function of the second kind of zero-order; and c_1 and c_2 are constants of integration. Applying the boundary conditions $\phi = 1$ at $r = r_p$, and $\phi = 0$ at $r = \infty$ to Eq. (22), the values of $c_1 = 0$ and $c_2 = 1/K_0\left(\beta r_p\right)$ are obtained. The solution of Eq. (17) leads to:

$$\phi = \frac{K_0\left(\beta r\right)}{K_0\left(\beta r_p\right)} \tag{23}$$

Subgrade reactions calculated by Eq. (15) and (16) are written as follows:

$$k_j = \frac{\pi r_p^2 G_k^* \beta^2}{K_0^2\left(\beta r_p\right)}\left[K_0\left(\beta r_p\right)K_2\left(\beta r_p\right) - K_1^2\left(\beta r_p\right)\right] - \pi r_p^2 \rho_j \omega^2 - \frac{\pi r_p^2 \rho_k \omega^2}{K_0^2\left(\beta r_p\right)}\left[K_1^2\left(\beta r_p\right) - K_0^2\left(\beta r_p\right)\right] \tag{24}$$

$$t_j = \frac{\pi r_p^2 \bar{E}_k^*}{K_0^2\left(\beta r_p\right)}\left[K_1^2\left(\beta r_p\right) - K_0^2\left(\beta r_p\right)\right] \tag{25}$$

6. DISPLACEMENT APPROXIMATION

Vertical displacement along a bar element is approximated by nodal displacements as the following equation (Fig. 1c):

$$U_{zj} = N_{1j} U_{z1j} + N_{2j} U_{z2j} \tag{26}$$

where U_{z1j} and U_{z2j} are vertical displacement at the first node and the second node of j^{th} pile element, respectively; N_{1j} and N_{2j} are shape functions that can be given the following forms:

$$N_{1j} = \frac{\cosh\left(\alpha_j z\right)\sinh\left(\alpha_j L_j\right)}{\sinh\left(\alpha_j L\right)} - \frac{\cosh\left(\alpha_j L_j\right)\sinh\left(\alpha_j z\right)}{\sinh\left(\alpha_j L\right)}$$
$$N_{2j} = \frac{\sinh\left(\alpha_j z\right)}{\sinh\left(\alpha_j L_j\right)} \tag{27}$$

where:

$$\alpha_j = \sqrt{\frac{k_j}{E_j^* A + t_j}} \tag{28}$$

Based on the approximation of displacement in Eq. (26), values of a and b are calculated as:

$$\begin{aligned} a &= \sum_{j=1}^{N} G_k^* \int_0^{L_j} \left(N_{1j} U_{z1j} + N_{2j} U_{z2j} \right)^2 dz \\ &= \sum_{j=1}^{N} \frac{G_k^*}{4\alpha_j \sinh^2\left(L_j\alpha_j\right)} \\ &\left\{ 4L_j\alpha_j U_{z1j} U_{z2j} \cosh\left(L_j\alpha_j\right) \right. \\ &-4U_{z1j} U_{z2j} \sinh\left(L_j\alpha_j\right) \\ &-\left(U_{z1j}^2 + U_{z2j}^2\right) 2L_j\alpha_j \\ &\left. +\left(U_{z1j}^2 + U_{z2j}^2\right) \sinh\left(2L_j\alpha_j\right) \right\} \end{aligned} \tag{29}$$

$$\begin{aligned} b &= \sum_{j=1}^{N} \bar{E}_k^* \int_0^{L_j} \left(\frac{dN_{1j}}{dz} U_{z1j} + \frac{dN_{2j}}{dz} U_{z2j} \right)^2 dz \\ &-\omega^2 \sum_{j=1}^{N} \rho_k \int_0^{L_j} \left(N_{1j} U_{z1j} + N_{2j} U_{z2j} \right)^2 dz \\ &= \sum_{j=1}^{N} \frac{\bar{E}_k^* \alpha_j}{4\sinh^2\left(L_j\alpha_j\right)} \\ &\left\{ -4L_j\alpha_j U_{z1j} U_{z2j} \cosh\left(L_j\alpha_j\right) \right. \\ &-4U_{z1j} U_{z2j} \sinh\left(L_j\alpha_j\right) \\ &+\left(U_{z1j}^2 + U_{z2j}^2\right) 2L_j\alpha_j \\ &\left. +\left(U_{z1j}^2 + U_{z2j}^2\right) \sinh\left(2L_j\alpha_j\right) \right\} \\ &-\omega^2 \sum_{j=1}^{N} \frac{\rho_k}{4\alpha_j \sinh^2\left(L_j\alpha_j\right)} \\ &\left\{ 4L_j\alpha_j U_{z1j} U_{z2j} \cosh\left(L_j\alpha_j\right) \right. \\ &-4U_{z1j} U_{z2j} \sinh\left(L_j\alpha_j\right) \\ &-\left(U_{z1j}^2 + U_{z2j}^2\right) 2L_j\alpha_j \\ &\left. +\left(U_{z1j}^2 + U_{z2j}^2\right) \sinh\left(2L_j\alpha_j\right) \right\} \end{aligned} \tag{30}$$

7. ITERATIVE SOLUTION

The iterative solution proposed by Nghiem and Chang [15] is employed in this study to solve Eq. (13). Consider the j[th] element as shown in Fig. 2, the equivalent impedance is defined as:

$$K_j = \frac{P_j}{U_{z1j}} \tag{31}$$

where P_j is the vertical load at the top of the j[th] element. All elements below the j[th] element (from j+1 to N) are modeled by a spring with an equivalent impedance of K_{j+1}. The spring is connected to the j[th] element at the second node, as shown in Fig. 2.

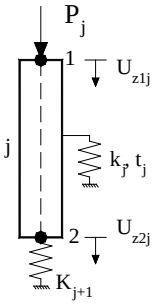

Fig. 2. Spring model of the j[th] element

Equation (14) can be written in the following matrix form by introducing Eq. (26) to Eq. (14):

$$s_j \frac{d^2}{dz^2} \begin{bmatrix} N_{1j} & N_{2j} \end{bmatrix} \begin{Bmatrix} U_{z1j} \\ U_{z2j} \end{Bmatrix} - k_j \begin{bmatrix} N_{1j} & N_{2j} \end{bmatrix} \begin{Bmatrix} U_{z1j} \\ U_{z2j} \end{Bmatrix} = 0 \tag{32}$$

where $s_j = E_j^* A + t_j$.

Applying Galerkin method and Green theory [17] to Eq. (32) leads to stiffness matrix of the j[th] element as follows:

$$\left[K\right]_j = s_j\alpha_j \begin{bmatrix} \dfrac{\cosh\left(\alpha_j L_j\right)}{\sinh\left(\alpha_j L_j\right)} & -\dfrac{1}{\sinh\left(\alpha_j L_j\right)} \\ -\dfrac{1}{\sinh\left(\alpha_j L_j\right)} & \dfrac{\cosh\left(\alpha_j L_j\right)}{\sinh\left(\alpha_j L_j\right)} \end{bmatrix} \tag{33a}$$

Equation (33a) can be written in the following form:

$$\left[K\right]_j = \begin{bmatrix} k_{11,j} & k_{12,j} \\ k_{21,j} & k_{22,j} \end{bmatrix} \tag{33b}$$

where $k_{11,j} = k_{22,j} = s_j\alpha_j \dfrac{\cosh\left(\alpha_j L_j\right)}{\sinh\left(\alpha_j L_j\right)}$

and $k_{12,j} = k_{21,j} = -s_j\alpha_j \dfrac{1}{\sinh\left(\alpha_j L_j\right)}$

The equilibrium equation for the j[th] element can be written as:

$$\left[K\right]_j \left\{U_z\right\}_j = \left\{P\right\}_j \tag{34}$$

where $\left\{U_z\right\}_j$ and $\left\{P\right\}_j$ are displacement and load vectors. The matrix form of Eq. (34) is obtained as:

$$\begin{bmatrix} k_{11,j} & k_{12,j} \\ k_{21,j} & k_{22,j} \end{bmatrix} \begin{Bmatrix} U_{z1j} \\ U_{z2j} \end{Bmatrix} = \begin{Bmatrix} P_j \\ -K_{j+1}U_{z2j} \end{Bmatrix} \tag{35}$$

The solution of Eq. (35) provides the displacement at the first and second nodes, as:

$$U_{z1j} = \frac{P_j}{k_{11,j} - \dfrac{k_{12,j}k_{21,j}}{k_{22,j}K_{j+1}}} \tag{36}$$

$$U_{z2j} = U_{z1j}\frac{k_{21,j}}{k_{22,j} + K_{j+1}} \tag{37}$$

Substituting Eq. (36) to Eq. (31), the flowing equation of the equivalent impedance of the j[th] element can be written:

$$K_j = k_{11,j} - \frac{k_{12,j}k_{21,j}}{k_{22,j}K_{j+1}} \tag{38}$$

Assumption can be made that the second node of the N[th] element is fixed, or $K_{N+1} = \infty$. The equivalent impedance of this element can be calculated from Eq. (38), as:

$$K_N = k_{11,N} \tag{39}$$

Iterating the calculations of the equivalent stiffness from the bottom element (the N[th] element) up to the top element (the 1[st] element) gives the equivalent impedance of all elements. As the definition in Eq. (31), the displacement at the pile head is calculated as:

$$U_{z0} = U_{z11} = \frac{P_1}{K_1} = \frac{P}{K_1} \tag{40}$$

Since the displacement of the second node of the (j-1)[th] element is equal to the displacement of the first node of the j[th] element ($U_{z2(j-1)} = U_{z1j}$), the displacement at the second node of the j[th] element is calculated by Eq. (37). The vertical load at the top of the j[th] element is also calculated at the same time as displacement using the following equation:

$$P_j = U_{z1j}K_j \tag{41}$$

The pile head impedance (or the impedance of the first element) can be expressed in terms of real (stiffness) and imaginary (damping) parts as:

$$K_1 = K_V + iC_V \tag{42}$$

where K_V is the pile head stiffness; and C_V is the pile head damping.

Fig. 3 shows the flow chart of the iterative solution scheme. The solution converged when the relative difference of β is less than a predefined tolerance, $\varepsilon = 0.000001$. The above theory and the Novak's method [1,3] are implemented in a computer code written by Delphi programming language to perform the analyses in this study.

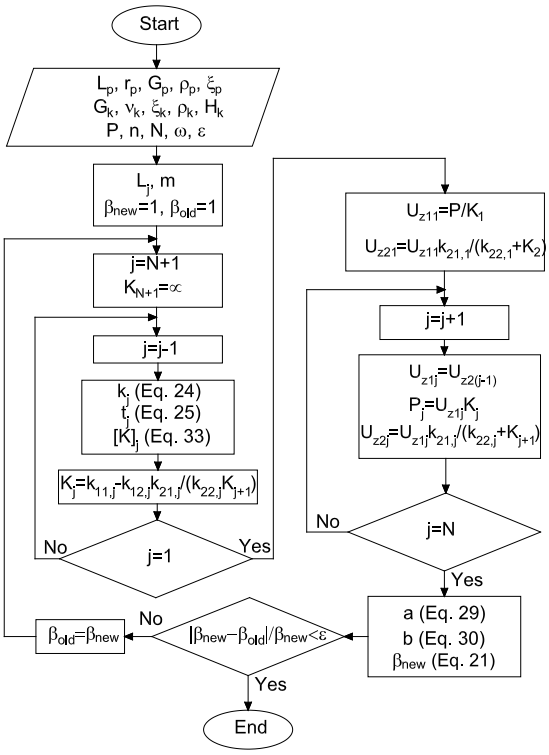

Fig. 3. Flow chart for the solution scheme

8. VALIDATION

8.1 End-bearing Pile

The proposed method is validated by comparing its analysis results with those from an approximate analytical method developed by Mylonakis [4] (the modified Novak's method) for dynamic analysis of axially loaded end-bearing pile. In both methods, the governing equation derived with assumption that soil displacement in the radial direction is zero as the restraint in radial direction is applied to the pile-soil system. As a result, the pile stiffness is overestimated. To overcome this shortcoming,

Mylonakis [4] replaced $\bar{E}_s^* = \lambda_s^* + 2G_s^*$ by $\bar{E}^* = \eta_s G_s^*$ where $\eta_s = 2/(1-\nu_s)$ and this modification is adopted in the analyses for comparison convenience. The pile and soil with L_p/r_p of 10, 14, and 20, E_p/E_s of 100, 300, and 1000, $\nu_s = 0.4$, $\rho_p/\rho_s = 1.25$, and $\xi_s = 0.05$ is used in the analyses. The normalized pile head stiffness, K_v/K_{v0} and pile head damping ratio, $C_v/(2K_v)$ are obtained from both methods, where K_{v0} is static pile head stiffness. As shown in Fig. 4, the normalized pile head stiffness and the pile head damping ratio are plotted versus dimensionless frequency, $a_0 = \omega/\left(r_p\sqrt{\rho_s/G_s}\right)$. Nearly similar results can be observed for both the methods. It is indicated that they produce identical dynamic subgrade reaction.

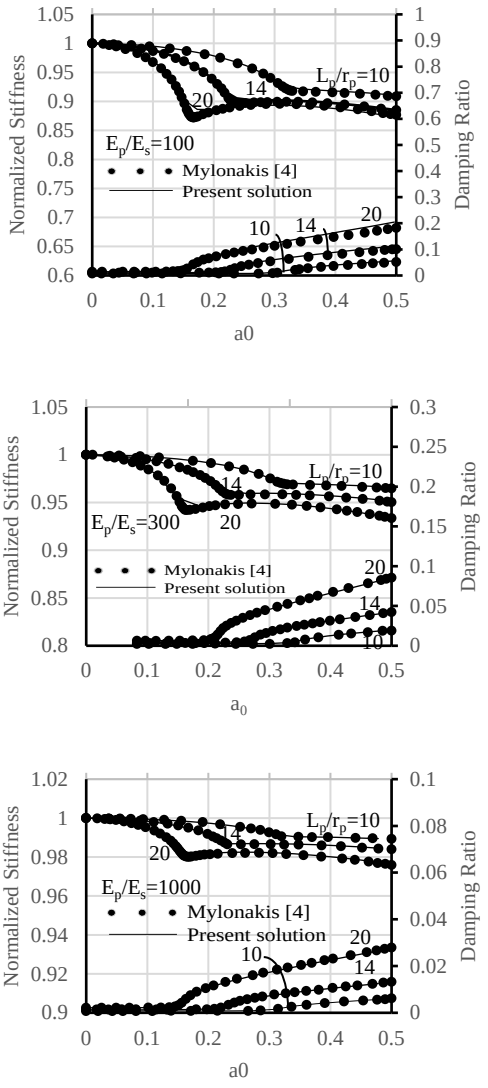

Fig. 4. Normalized stiffness and damping ratio versus dimensionless frequency of end-bearing piles

7.2 Friction Pile

A friction pile with slenderness ratio of $L_p/r_p = 50$ is embedded in a homogeneous soil media. The ratios of pile and soil properties are selected as E_p/E_s of 100, 300, and 1000, and $\rho_p/\rho_s = 1.25$. Other soil properties are constants in all analyses such as Poison's ratio, $\nu_s = 0.3$, and soil damping ratio, $\xi_s = 0.05$. The energy principles and variational approach (EPVA) and the Novak's method (NM) [1,3] are used in the analyses. The effect of radial restraint is reduced by using the modification moduli proposed by Seo et al. [12] where the moduli λ_s^* and G_s^* of the soil were replaced by $\bar{\lambda}_s^* = 0$ and $\bar{G}_s^* = 0.75G_s\left(1+1.25\nu_s^2\right)$, respectively.

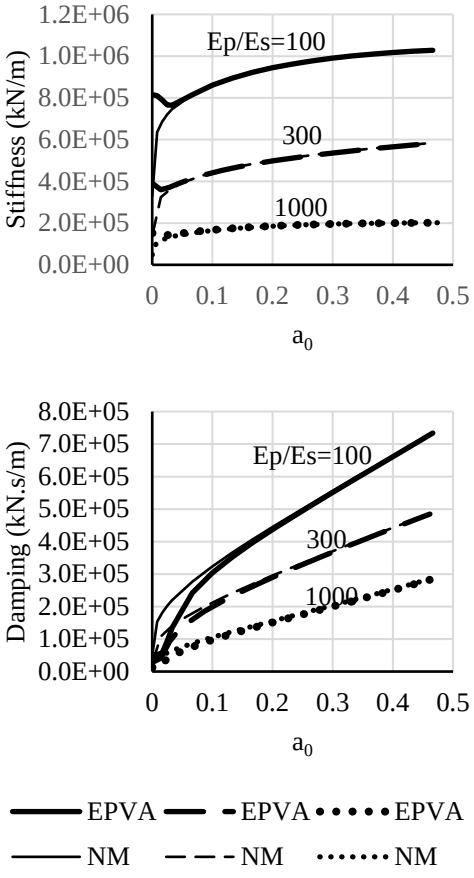

Fig. 5. Pile head impedance versus dimensionless frequency of friction pile in homogeneous soil

Fig. 5 shows the pile head stiffness and damping versus dimensionless frequency a_0 for both methods. The pile head impedances match perfectly for stiffness with $a_0 > 0.03$ and for damping with $a_0 > 0.1$. At zero frequency, the subgrade reaction

in the NM is also zero [3] so the NM is unable to provide static pile head stiffness. This characteristic also explains why large differences of the pile head impedances occurred at low frequencies as shown in Fig. 5. Table 1 presented the pile head stiffnesses obtained from the EPVA and compared to those from the 3D finite element method (3DFEM) using SSI3D program [18]. The absolute values of relative differences between the EPVA and 3DFEM are found in range of 2.9% to 11.3%.

Table 1 The static pile head stiffness (kN/m) for friction pile in homogeneous soil

Case	EPVA	3DFEM	Differences (%)
$E_p/E_s=100$	814540	838000	-2.9
$E_p/E_s=300$	390130	422246	-8.2
$E_p/E_s=1000$	151960	169183	-11.3

A single pile is embedded in three idealized multi-layered soil profiles with configuration of geometry is shown in Fig. 6 and Table 2. The analyses are conducted using the EPVA and NM with pile slenderness ratio of $L_p/r_p=25$. The analyses using 3DFEM are also performed to verify the static pile head stiffness obtained from the EPVA. Fig. 7 plots the pile head stiffness and damping versus dimensionless frequency $a_0=\omega/\left(r_p\sqrt{\rho_1/G_1}\right)$ for both methods. The second analysis case provide highest pile head stiffness and damping at high frequencies. The results of pile head stiffness are in good agreement for $a_0>0.1$ while high discrepancies of the pile head damping are observed with values of a_0 vary from 0 to 0.4. The EPVA provides more accurate results than the NM because the normal stress component in the vertical direction is considered in EPVA while it was ignored in the NM.

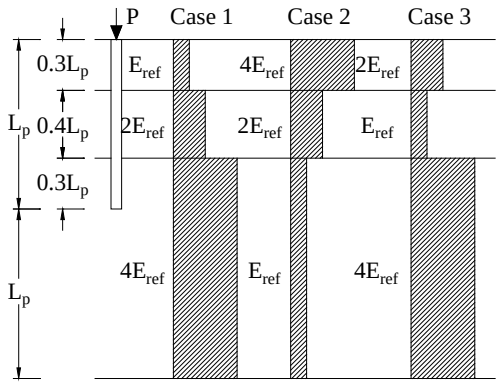

Fig. 6. Analysis cases for friction pile in layered soil

Table 2 Analysis cases for friction pile in layered soil

Layer No.	Case 1	Case 2	Case 3
	E_k/E_{ref}		
1	1.0	4.0	2.0
2	2.0	2.0	1.0
3	4.0	1.0	4.0

Table 3 The static pile head stiffness (kN/m) for friction pile in layered soil

Case	EPVA	3DFEM	Differences (%)
1	1174550	1317518	-12.2
2	1152340	1125578	2.3
3	1202810	1293134	-7.5

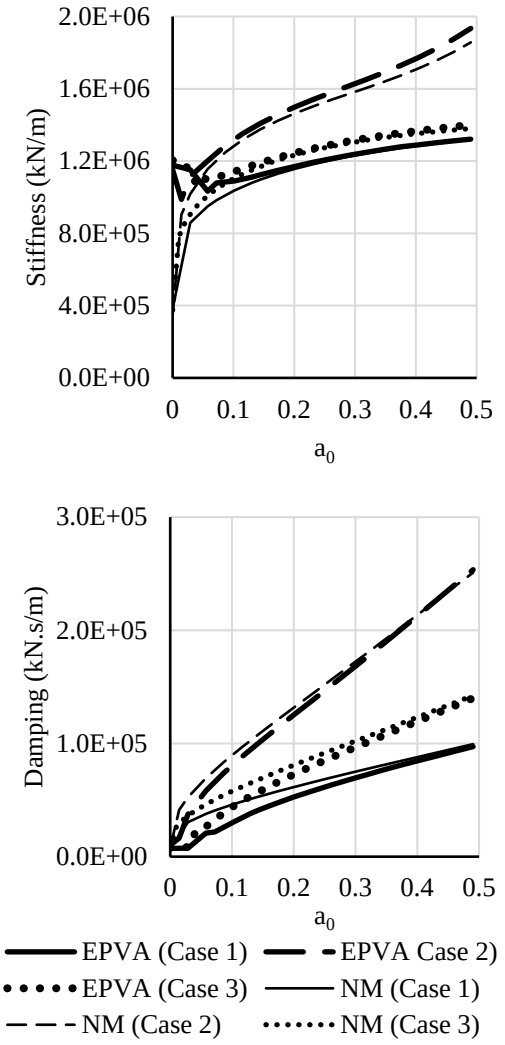

Fig. 7. Pile head impedance versus dimensionless frequency of friction pile in layered soil

The pile head stiffnesses obtained from the EPVA and compared to those from the 3DFEM with differences in range of -12.2% to 2.3% as presented in Table 3. The differences mainly depend on the use of the reduction modulus equation proposed by Seo et al. [12] accounted for the effect of restraint in the radial direction.

9. CONCLUSIONS

The vertical dynamic response of end-bearing and friction piles with circular cross-sections embedded in multi-layered soil was investigated. Based on the comparison of the analysis results with the modified Novak's method, the NM method and the 3D finite element method, the following conclusions are obtained:

1) Both normal and shear strains in the vertical direction are considered in the energy principles and variational approach.
2) The proposed solution produces the pile head impedance in excellent agreement in comparison to that from the modified Novak's method for the end-bearing pile.
3) The proposed solution can predict static and dynamic pile head stiffness while Novak's method is unable to provide the static stiffness and underestimate the dynamic stiffness at a low frequency for friction pile.

10. REFERENCES

[1] Novak M., Dynamic Stiffness and Damping of Piles, Canadian Geotechnical Journal, Vol. 11, 1974, pp. 574-598.

[2] Lakshmanan N., and Minai R., Dynamic Soil Reactions in Radially Non-Homogeneous Soil Media, Bulletin of the Disaster Prevention Research Institute, Vol. 31, Issue 2, 1981, pp. 79-114.

[3] El Naggar M.H., Vertical and torsional soil reactions for radially inhomogeneous soil layer, Structural Engineering and Mechanics, Vol. 10, Issue 4, 2000, pp. 299–312.

[4] Mylonakis G., Elastodynamic model for large-diameter end-bearing shafts, Soils and Foundations, Vol. 41, Issue 3, 2001, pp. 31-44.

[5] Anoyatis G., and Mylonakis G., Dynamic Winkler modulus for axially loaded piles, Geotechnique, Vol. 62, No. 6, 2012, pp. 521–536.

[6] Randolph M.F., and Wroth C.P., Analysis of deformation of vertically loaded piles, Journal of Geotechnical Engineering, ASCE, Vol. 104, No. 12, 1978, pp. 1465–1488.

[7] Rajapakse R.K., and Shah A.H., On the longitudinal harmonic motion of an elastic bar embedded in an elastic half-space, International Journal of Solids and Structures, Vol. 23, Issue 2, 1987, pp. 267-85.

[8] Rajapakse R.K., and Shah A.H., Impedance curves for an elastic pile, Soil Dynamics and Earthquake Engineering, Vol. 8, Issue 3, 1989, pp. 145-52.

[9] Rajapakse R.K., A note on the elastodynamic load transfer problem, International journal of solids and structures, Vol. 24, Issue 9, 1988, pp. 963-972.

[10] Vallabhan C.V.G., and Mustafa G., A new model for the analysis of settlement of drilled piers, International Journal for Numerical and Analytical Methods in Geomechanics, Vol. 20, Issue 2, 1996, pp. 143-152.

[11] Seo H., and Prezzi M., Analytical solutions for a vertically loaded pile in multilayered soil, Geomechanics and Geoengineering: An International Journal, Vol.2, Issue 1, 2007, pp. 51-60.

[12] Seo H., Basu D., Prezzi M., and Salgado R., Load-Settlement Response of Rectangular and Circular Piles in Multilayered Soil, Journal of Geotechnical and Geoenvironmental Engineering, Vol.135, Issue 3, 2008, pp. 420-430.

[13] Salgado R., Seo H., Basu D., and Prezzi M., Variational elastic solution for axially loaded piles in multilayered soil, International Journal for Numerical and Analytical Methods in Geomechanics, Vol.37, 2013, pp. 423–440.

[14] Gupta B.K., and Basu D., Dynamic analysis of axially loaded end-bearing pile in a homogeneous viscoelastic soil, Soil Dynamics and Earthquake Engineering, Vol. 111, 2018, pp. 31-40.

[15] Nghiem H.M., and Chang N.Y., Efficient solution for a single pile under torsion, Soils and Foundations, Vol. 59, 2019, pp. 13-26.

[16] Kramer S.L., Geotechnical earthquake engineering, Vol. xviii, Upper Saddle River, NJ: Prentice Hall, 1996.

[17] Smith I.M., Griffiths D.V., Programming the finite element method, Fourth Edition, John Wiley & Sons, 2004.

[18] Nghiem H.M., Soil-pile-structure interaction effects of highrise building under seismic shaking, Dissertation, University of Colorado Denver, 2009.